An Analytical Approach in Analysis of Local Oscillator Near-the-Carrier AM Noise Suppression in Microwave Balanced Mixers

Ali Kheirdoost, Ali Banai, *Member, IEEE*, and Forouhar Farzaneh, *Senior Member, IEEE*

***Abstract*—In this paper, a new formulation based on conversion matrix method is proposed to analyze "near-the-carrier local ocillator (LO) noise" down conversion to IF in microwave mixers. This method could be easily applied to analyze LO noise down conversion in any type of mixer. Practical results of this method have been compared with the envelope method and measurement results. It is shown that despite the conventional AM noise suppression in balanced mixers, the near-the-carrier LO noise suppression does not occur necessarily at the center frequency of hybrid in balanced mixers. AM noise suppression values are predicted precisely.**

***Index Terms*—AM noise, balanced mixers, conversion matrix, microwave mixers, mixer noise.**

I. Introduction

SENSITIVITY of a receiver mixer is usually limited by its internally generated noise sources. One of these sources is the noise injected into the mixer along with the local oscillator (LO) signal [1]. As stated in the literature in balanced mixers, mostly the AM component of LO noise is rejected and just the phase noise is down converted into the IF. LO AM noise is referred to as the noise whose components are located in RF and image frequencies and we will call it "far-from-the-carrier noise." As an example, the spectrum of an oscillator with this noise is depicted in Fig. 1. This is the so-called AM noise in balanced mixers, which due to the symmetry of mixer is suppressed [2].

In some applications, especially in millimeter waves, it is needed to use frequency multipliers and amplifiers to provide LO signal in the desired frequency. These amplifier and frequency multiplier stages result in noisy LO sources that would have components in RF and image frequencies. In cases where LO and RF frequency distance is high enough, using a high-Q filter in the final stage of the LO source far from carrier noise components in RF and image frequencies could be easily reduced [1]. Here, we describe "near-the-carrier noise" as the LO noise whose components are nearer than RF and image frequencies to the LO (as depicted in Fig. 2).

Although modern phase-locked oscillators have low near-the-carrier AM noise, but in inexpensive systems such as automotive anticollision radars, in which simple free-running millimeter-wave voltage-controlled oscillators (VCOs) are used, the AM near-the-carrier noise suppression can improve system performance significantly [3].

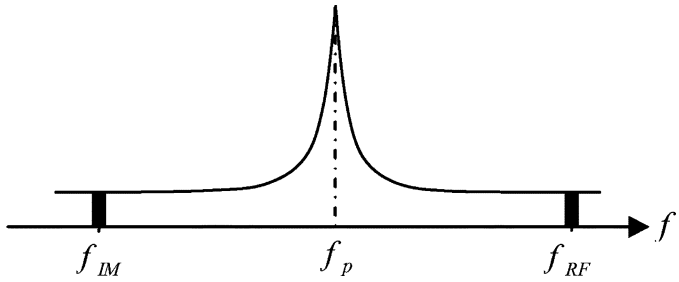

Fig. 1. Far-from-the-carrier LO noise spectrum components.

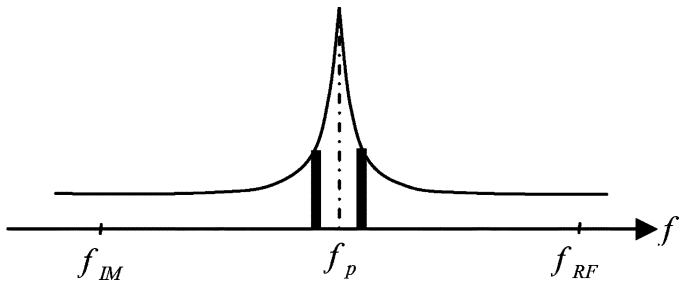

Fig. 2. LO near-the-carrier noise spectrum components.

Contrary to LO far-from-the-carrier noise, near-the-carrier LO noise mixing with RF signals results in IF noisy sidebands. Analysis of near-the-carrier LO noise in mixers could be easily applied to analysis of any type of near-the-carrier noise.

In the analysis of noise temperature of mixers, authors usually include the thermal noise source of constituent elements, and the noise temperature is calculated using these sources [4], [5]. Furthermore, in the literature, the noise cancellation techniques in microwave mixers have been studied [6], [7]. The effect of near-the-carrier LO noise in the measurement of phase noise in mixers has been studied as well and practical results have been reported [8], but it has not been reported whether near-the-carrier LO noise in each type of mixer is rejected or not. In [9], a general approach for noise analysis in multitone nonlinear circuits has been proposed. Although this method is general, it did not address the near-the-carrier AM noise suppression. Rejection of the AM component LO noise in balanced mixers in the literature is referred to as the LO noise, but we call it far-from-the-carrier LO noise in this paper.

Manuscript received September 03, 2008; revised December 17, 2008. First published March 16, 2009; current version published April 08, 2009.

The authors are with the School of Electrical Engineering, Sharif University of Technology, Tehran 11155-4363, Iran.

Color versions of one or more of the figures in this paper are available online at http://ieeexplore.ieee.org.

Digital Object Identifier 10.1109/TMTT.2009.2015106

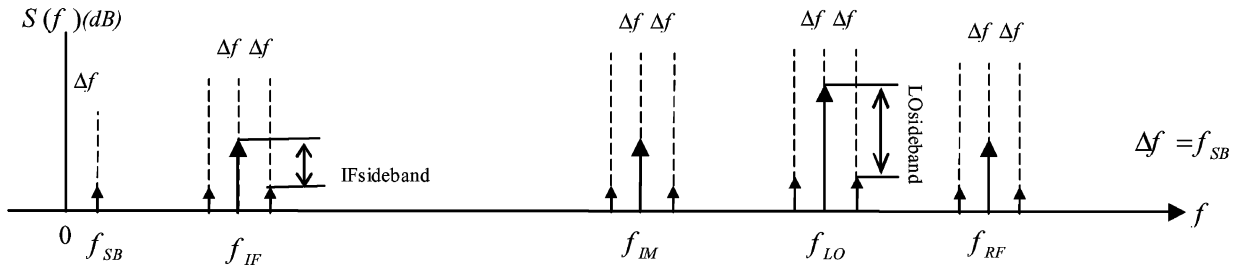

Fig. 3. New formulation's harmonics.

In this paper, the phenomenon of near-the-carrier LO noise rejection or down conversion will be studied. Different methods for analysis [10], [12], [13] and synthesis [11], [14] of nonlinear circuits under different driving conditions have been proposed, but for our application, a novel method based on Taylor expansion of nonlinear elements, similar to conversion matrix method, is proposed. This method can be considered as an extension of the conversion matrix method.

In this paper, we will represent LO near-the-carrier noise in the form of harmonics at frequencies $f_p + f_{\rm SB}$ and $f_p - f_{\rm SB}$, and the process of down conversion of these frequencies to IF will be studied.

II. Theory

As stated earlier, LO near-the-carrier noise sidebands will be presented using two deterministic signals, similar to noise analysis using a conversion matrix [15]. In simulation and measurement steps, the LO sidebands are considered as AM or PM excitations, and sidebands at other frequencies are responses of the circuit to those excitations. Corresponding harmonics present in the analysis of near-the-carrier noise in mixers are depicted in Fig. 3.

In analysis of far-from-the-carrier LO noise, the conversion matrix method is a helpful tool because LO noise mixing with the LO carrier results in IF noise that has been targeted to be studied [14], but near-the-carrier LO noise down conversion to IF frequency is the result of the mixing with the RF signal, and thus, the conventional conversion matrix formulation will not help in the analysis of this process. As such, a generalized conversion matrix (GCM) method will be proposed as a novel analytical tool in the analysis of the LO noise down conversion. Similar to the classic conversion matrix method, we will use a double-sided spectrum, but for computations, only upper sidebands of noise will be sufficient to be included in the formulation.

As we know, noise down conversion is the result of the mixing in nonlinear elements of the mixer so we first need to model the nonlinear elements in the presence of these harmonics, and then by modeling linear elements, all the circuits could be easily studied.

A. Nonlinear Conductance

We represent the nonlinear conductance equation in the time domain as

$$i = f(v). \tag{1}$$

As we know, the time-domain voltage is the sum of all components depicted in Fig. 3. Thus, we can write

$$v = v_p + v_n + v_{{\rm SB}n} + v_{{\rm SB}p}. \tag{2}$$

In which v_p is the pump or LO signal and its harmonics in the time domain, v_n is the sum of signals at frequencies $n\omega_p \pm \omega_0$, $v_{{\rm SB}n}$ is the sum of harmonics at frequencies $n\omega_p \pm \omega_0 + \omega_{\rm SB}$, and $v_{{\rm SB}p}$ is the sum of harmonics at frequencies $n\omega_p + \omega_{\rm SB}$. Here, ω_p, ω_0 and $\omega_{\rm SB}$ are pump frequency, IF frequency, and sidebands offset from the LO, respectively. The same definition stands for currents at different frequencies.

Thus, we have

$$i = f(v_p + v_n + v_{{\rm SB}n} + v_{{\rm SB}p}). \tag{3}$$

By Taylor expansion of this equation, we will have

$$i \cong f(v_p) + \left.\frac{\partial f(v)}{\partial v}\right|_{v=v_p} (v_n + v_{{\rm SB}n} + v_{{\rm SB}p}) + \frac{1}{2!}\left.\frac{\partial^2 f(v)}{\partial v^2}\right|_{v=v_p} (v_n + v_{{\rm SB}n} + v_{{\rm SB}p})^2. \tag{4}$$

The resultant terms and their frequencies are listed in Table I and, thus, the formulation can be arranged more as shown in Table I.

As can be deduced from Table I, for our formulation terms 5–7, 9, and 10 generate harmonics that are small enough and can be neglected in the analysis. The remaining terms should be included in the formulation.

Thus, by arranging (4) and focusing on sideband terms, we would have

$$\begin{aligned} i_{{\rm SB}n} + i_{{\rm SB}p} &= \left.\frac{\partial f(v)}{\partial v}\right|_{v=v_p} (v_{{\rm SB}n} + v_{{\rm SB}p}) \\ &\quad + \left.\frac{\partial^2 f(v)}{\partial v^2}\right|_{v=v_p} v_n (v_{{\rm SB}p} + v_{{\rm SB}n}) \\ &= \left(\left.\frac{\partial f(v)}{\partial v}\right|_{v=v_p} + y_n \right) (v_{{\rm SB}n} + v_{{\rm SB}p}) \end{aligned} \tag{5}$$

in which y_n is defined as

$$y_n = \left.\frac{\partial^2 f(v)}{\partial v^2}\right|_{v=v_p} v_n. \tag{6}$$

y_n includes harmonics in frequencies $n\omega_p \pm \omega_0$ and can be calculated using a simple conversion matrix analysis.

TABLE I
TAYLOR EXPANSION HARMONICS

No.	Expansion Term	Frequency
1	$f(v_p)$	$n\omega_p$
2	$\left(\left.\frac{\partial f(v)}{\partial v}\right\|_{v=v_p}\right)v_n$	$n\omega_p \pm \omega_0$
3	$\left(\left.\frac{\partial f(v)}{\partial v}\right\|_{v=v_p}\right)v_{SBp}$	$n\omega_p + \omega_{SB}$
4	$\left(\left.\frac{\partial f(v)}{\partial v}\right\|_{v=v_p}\right)v_{SBn}$	$n\omega_p \pm \omega_0 + \omega_{SB}$
5	$\frac{1}{2}\left(\left.\frac{\partial^2 f(v)}{\partial v^2}\right\|_{v=v_p}\right)v_n^2$	$n\omega_p \pm 2\omega_0$
6	$\frac{1}{2}\left(\left.\frac{\partial^2 f(v)}{\partial v^2}\right\|_{v=v_p}\right)v_{SBp}^2$	$n\omega_p + 2\omega_{SB}$
7	$\frac{1}{2}\left(\left.\frac{\partial^2 f(v)}{\partial v^2}\right\|_{v=v_p}\right)v_{SBn}^2$	$n\omega_p \pm 2\omega_0 + 2\omega_{SB}$
8	$\left(\left.\frac{\partial^2 f(v)}{\partial v^2}\right\|_{v=v_p}\right)v_n v_{SBp}$	$n\omega_p \pm \omega_0 + \omega_{SB}$
9	$\left(\left.\frac{\partial^2 f(v)}{\partial v^2}\right\|_{v=v_p}\right)v_n v_{SBn}$	$n\omega_p \pm 2\omega_0 + \omega_{SB}$ / $n\omega_p + \omega_{SB}$
10	$\left(\left.\frac{\partial^2 f(v)}{\partial v^2}\right\|_{v=v_p}\right)v_{SBp}v_{SBn}$	$n\omega_p \pm \omega_0 + 2\omega_{SB}$

Noting that

$$\left.\frac{\partial f(v)}{\partial v}\right|_{v=v_p} = \sum_{n=-N}^{N} F'_n e^{jn\omega_p t} \tag{7}$$

and

$$i_{\mathrm{SB}n1} = \sum_{n=-N}^{N} I_{n,1,1} e^{j(n\omega_p+\omega_0+\omega_{\mathrm{SB}})t} \tag{8}$$

$$v_{\mathrm{SB}n1} = \sum_{n=-N}^{N} V_{n,1,1} e^{j(n\omega_p+\omega_0+\omega_{\mathrm{SB}})t} \tag{9}$$

$$i_{\mathrm{SB}n2} = \sum_{n=-N}^{N} I_{n,-1,1} e^{j(n\omega_p-\omega_0+\omega_{\mathrm{SB}})t} \tag{10}$$

$$v_{\mathrm{SB}n2} = \sum_{n=-N}^{N} V_{n,-1,1} e^{j(n\omega_p-\omega_0+\omega_{\mathrm{SB}})t} \tag{11}$$

$$i_{\mathrm{SB}p} = \sum_{n=-N}^{N} I_{n,0,1} e^{j(n\omega_p+\omega_{\mathrm{SB}})t} \tag{12}$$

$$v_{\mathrm{SB}p} = \sum_{n=-N}^{N} V_{n,0,1} e^{j(n\omega_p+\omega_{\mathrm{SB}})t} \tag{13}$$

$$y_n = \sum_{n=-N}^{N} \left[Y_n e^{j(n\omega_p+\omega_0)t} + Y_n^* e^{-j(n\omega_p+\omega_0)t} \right]. \tag{14}$$

By rearranging (5) at different frequency components, we will achieve the following matrix relations:

$$\mathbf{I_{SBn1}} = \mathbf{F}\mathbf{V_{SBn1}} + \mathbf{Y}\mathbf{V_{SBp}} \tag{15}$$

$$\mathbf{I_{SBn2}} = \mathbf{F}\mathbf{V_{SBn2}} + \mathbf{Y}'\mathbf{V_{SBp}} \tag{16}$$

$$\mathbf{I_{SBp}} = \mathbf{Y}'\mathbf{V_{SBn1}} + \mathbf{Y}\mathbf{V_{SBn2}} + \mathbf{F}\mathbf{V_{SBp}} \tag{17}$$

in which $\mathbf{Y}'$ deotes the transpose conjugate of matrix $\mathbf{Y}$ and where other terms are as follows:

$$\mathbf{F} = \begin{bmatrix} F'_0 & F'_{-1} & \cdots & F'_{-2N+1} & F'_{-2N} \\ F'_1 & F'_0 & \cdots & F'_{-2N+2} & F'_{-2N+1} \\ \vdots & \vdots & \ddots & \vdots & \vdots \\ F'_{2N-1} & F'_{2N-2} & \cdots & F'_0 & F'_{-1} \\ F'_{2N} & F'_{2N-1} & \cdots & F'_1 & F'_0 \end{bmatrix} \tag{18}$$

$$\mathbf{Y} = \begin{bmatrix} Y_0 & Y_{-1} & \cdots & Y_{-2N+1} & Y_{-2N} \\ Y_1 & Y_0 & \cdots & Y_{-2N+2} & Y_{-2N+1} \\ \vdots & \vdots & \ddots & \vdots & \vdots \\ Y_{2N-1} & Y_{2N-2} & \cdots & Y_0 & Y_{-1} \\ Y_{2N} & Y_{2N-1} & \cdots & Y_1 & Y_0 \end{bmatrix} \tag{19}$$

$$\mathbf{V_{SBn1}} = \begin{bmatrix} V_{-N,1,1} \\ \vdots \\ V_{0,1,1} \\ \vdots \\ V_{N,1,1} \end{bmatrix} \quad \mathbf{I_{SBn1}} = \begin{bmatrix} I_{-N,1,1} \\ \vdots \\ I_{0,1,1} \\ \vdots \\ I_{N,1,1} \end{bmatrix} \tag{20}$$

$$\mathbf{V_{SBn2}} = \begin{bmatrix} V_{-N,-1,1} \\ \vdots \\ V_{0,-1,1} \\ \vdots \\ V_{N,-1,1} \end{bmatrix} \quad \mathbf{I_{SBn2}} = \begin{bmatrix} I_{-N,-1,1} \\ \vdots \\ I_{0,-1,1} \\ \vdots \\ I_{N,-1,1} \end{bmatrix} \tag{21}$$

$$\mathbf{V_{SBp}} = \begin{bmatrix} V_{-N,0,1} \\ \vdots \\ V_{0,0,1} \\ \vdots \\ V_{N,0,1} \end{bmatrix} \quad \mathbf{I_{SBp}} = \begin{bmatrix} I_{-N,0,1} \\ \vdots \\ I_{0,0,1} \\ \vdots \\ I_{N,0,1} \end{bmatrix}. \tag{22}$$

Furthermore, by arranging (15)–(17) in a compact matrix form, we arrive at (23) as follows:

$$\begin{bmatrix} \mathbf{I_{SBn1}} \\ \mathbf{I_{SBn2}} \\ \mathbf{I_{SBp}} \end{bmatrix} = \begin{bmatrix} \mathbf{F} & \mathbf{0} & \mathbf{Y} \\ \mathbf{0} & \mathbf{F} & \mathbf{Y}' \\ \mathbf{Y}' & \mathbf{Y} & \mathbf{F} \end{bmatrix} \begin{bmatrix} \mathbf{V_{SBn1}} \\ \mathbf{V_{SBn2}} \\ \mathbf{V_{SBp}} \end{bmatrix}. \tag{23}$$

This way, for a nonlinear conductance, an admittance form GCM has been extracted and it could be used in relating noise currents to noise voltages in a nonlinear conductance.

B. Nonlinear Capacitance

Similarly we represent a nonlinear capacitive element in the time domain as

$$q = Q(v). \tag{24}$$

According to (2), we would have

$$i = \frac{d}{dt}Q(v_p + v_n + v_{\mathrm{SB}n} + v_{\mathrm{SB}p}). \tag{25}$$

In a similar fashion, using Taylor expansion and considering the frequencies of interest as in (5), we would have

$$\begin{aligned} i = {} & \frac{d}{dt}[Q(v_p)] + \frac{d}{dt}\left[\left.\frac{\partial Q}{\partial v}\right|_{v=v_p} v_n\right] \\ & + \frac{d}{dt}\left[\left.\frac{\partial Q}{\partial v}\right|_{v=v_p} (v_{\mathrm{SB}n} + v_{\mathrm{SB}p}) \right. \\ & \left. + \left.\frac{\partial^2 Q}{\partial v^2}\right|_{v=v_p} v_n(v_{\mathrm{SB}n} + v_{\mathrm{SB}p})\right]. \end{aligned} \tag{26}$$

Again, y_n is defined appropriately for a capacitive element as follows:

$$y_n = \left.\frac{\partial^2 Q}{\partial v^2}\right|_{v=v_p} v_n. \tag{27}$$

This includes terms at frequencies $n\omega_p \pm \omega_0$ and can be easily calculated using a simple conversion matrix analysis.

Now noting

$$\frac{\partial Q(v)}{\partial v_p} = \sum_{n=-N}^{N} Q'_n e^{jn\omega_p t}. \tag{28}$$

Using (8)–(13) and modifying (14) using (27), we will have again

$$y_n = \sum_{n=-N}^{N} (Y_n e^{j\omega_n t} + Y_n^* e^{-j\omega_n t}). \tag{29}$$

Furthermore, equating similar frequencies in relation (26), our new extended conversion matrix formulation for nonlinear capacitive element will be

$$\mathbf{I_{SBn1}} = j\mathbf{\Omega_{SBn1}}\mathbf{Q}\mathbf{V_{SBn1}} + j\mathbf{\Omega_{SBn1}}\mathbf{Y}\mathbf{V_{SBp}} \tag{30}$$

$$\mathbf{I_{SBn2}} = j\mathbf{\Omega_{SBn2}}\mathbf{Q}\mathbf{V_{SBn2}} + j\mathbf{\Omega_{SBn2}}\mathbf{Y'}\mathbf{V_{SBp}} \tag{31}$$

$$\begin{aligned} \mathbf{I_{SBp}} = {} & j\mathbf{\Omega_{SBp}}\mathbf{Y'}\mathbf{V_{SBn1}} + j\mathbf{\Omega_{SBp}}\mathbf{Y}\mathbf{V_{SBn2}} \\ & + j\mathbf{\Omega_{SBp}}\mathbf{Q}\mathbf{V_{SBp}} \end{aligned} \tag{32}$$

where

$$\mathbf{Q} = \begin{bmatrix} Q'_0 & Q'_{-1} & \cdots & Q'_{-2N+1} & Q'_{-2N} \\ Q'_1 & Q'_0 & \cdots & Q'_{-2N+2} & Q'_{-2N+1} \\ \vdots & \vdots & \ddots & \vdots & \vdots \\ Q'_{2N-1} & Q'_{2N-2} & \cdots & Q'_0 & Q'_{-1} \\ Q'_{2N} & Q'_{2N-1} & \cdots & Q'_1 & Q'_0 \end{bmatrix} \tag{33}$$

$$\mathbf{Y} = \begin{bmatrix} Y_0 & Y_{-1} & \cdots & Y_{-2N+1} & Y_{-2N} \\ Y_1 & Y_0 & \cdots & Y_{-2N+2} & Y_{-2N+1} \\ \vdots & \vdots & \ddots & \vdots & \vdots \\ Y_{2N-1} & Y_{2N-2} & \cdots & Y_0 & Y_{-1} \\ Y_{2N} & Y_{2N-1} & \cdots & Y_1 & Y_0 \end{bmatrix} \tag{34}$$

and matrices $\mathbf{\Omega_{SBn1}}, \mathbf{\Omega_{SBn2}}$ and $\mathbf{\Omega_{SBp}}$ are diagonal matrices similar to matrix $\mathbf{\Omega}$ in the conversion matrix approach defined as

$$\mathbf{\Omega_{SBn1}} = \begin{bmatrix} -N\omega_p + \omega_0 + \omega_{\mathrm{SB}} & \cdots & 0 \\ \vdots & \ddots & \vdots \\ 0 & \cdots & N\omega_p + \omega_0 + \omega_{\mathrm{SB}} \end{bmatrix} \tag{35}$$

$$\mathbf{\Omega_{SBn2}} = \begin{bmatrix} -N\omega_p - \omega_0 + \omega_{\mathrm{SB}} & \cdots & 0 \\ \vdots & \ddots & \vdots \\ 0 & \cdots & N\omega_p - \omega_0 + \omega_{\mathrm{SB}} \end{bmatrix} \tag{36}$$

$$\mathbf{\Omega_{SBp}} = \begin{bmatrix} -N\omega_p + \omega_{\mathrm{SB}} & \cdots & 0 \\ \vdots & \ddots & \vdots \\ 0 & \cdots & N\omega_p + \omega_{\mathrm{SB}} \end{bmatrix}. \tag{37}$$

Finally, by arranging (30)–(32) in a compact matrix form, (38) will be extracted as follows:

$$\begin{bmatrix} \mathbf{I_{SBn1}} \\ \mathbf{I_{SBn2}} \\ \mathbf{I_{SBp}} \end{bmatrix} = j\left(\begin{bmatrix} \mathbf{\Omega_{SBn1}} & \mathbf{0} & \mathbf{0} \\ \mathbf{0} & \mathbf{\Omega_{SBn2}} & \mathbf{0} \\ \mathbf{0} & \mathbf{0} & \mathbf{\Omega_{SBp}} \end{bmatrix} \times \begin{bmatrix} \mathbf{Q} & \mathbf{0} & \mathbf{Y} \\ \mathbf{0} & \mathbf{Q} & \mathbf{Y'} \\ \mathbf{Y'} & \mathbf{Y} & \mathbf{Q} \end{bmatrix} \begin{bmatrix} \mathbf{V_{SBn1}} \\ \mathbf{V_{SBn2}} \\ \mathbf{V_{SBp}} \end{bmatrix}\right). \tag{38}$$

As such, for a nonlinear capacitance, GCM admittance has been extracted.

C. Linear Elements

In general, for a linear element, GCM admittance will be as follows:

$$\begin{bmatrix} \mathbf{I_{SBn1}} \\ \mathbf{I_{SBn2}} \\ \mathbf{I_{SBp}} \end{bmatrix} = \begin{bmatrix} \mathbf{Y_{SBn1}} & \mathbf{0} & \mathbf{0} \\ \mathbf{0} & \mathbf{Y_{SBn2}} & \mathbf{0} \\ \mathbf{0} & \mathbf{0} & \mathbf{Y_{SBp}} \end{bmatrix} \begin{bmatrix} \mathbf{V_{SBn1}} \\ \mathbf{V_{SBn2}} \\ \mathbf{V_{SBp}} \end{bmatrix} \tag{39}$$

in which $\mathbf{Y_{SBn1}}, \mathbf{Y_{SBn2}}$ and $\mathbf{Y_{SBp}}$ are diagonal matrices whose main diagonal elements are admittances at corresponding frequencies [these frequencies are the same as those of elements of matrices (35)–(37)]. By combining the linear circuit and the nonlinear elements using these relations, the circuit analysis of a mixer could be easily performed and near-the-carrier noise down conversion could be studied. We have implemented this method for sideband noise calculations in a number of examples, two of which are presented here.

III. Mixer Design, Simulation, and Measurement

Two balanced mixers using a rat-race and a branch-line coupler at center frequency of 2 GHz have been designed and built. A diode matching network in arms of couplers for the best conversion performance of the mixer has been added. LO power of these mixers is set at 9 dBm and RF power is -10 dBm at a frequency of 10 MHz above LO frequency.

All simulations have been performed using Agilent's ADS software, as well as our GCM method implemented using MATLAB. Also in our simulations, noisy sidebands are considered in frequencies 10 kHz above and below LO. These mixers

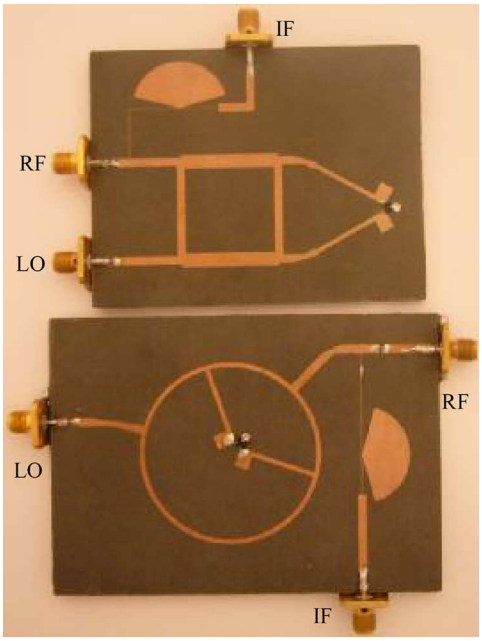

Fig. 4. Fabricated balanced mixers at the center frequency of 2 GHz.

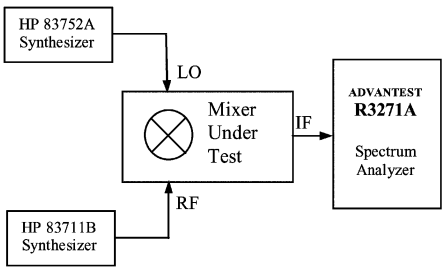

Fig. 5. Measurement setup used.

have been fabricated using Aglient's HSMS-8102 diodes, which are in a SOT-23 package, and because of this, the arms of couplers have been bended so that this package diode could be easily soldered on the printed circuit board (PCB) (Fig. 4). A single diode mixer using this diode has been also simulated by both programs. Measurement setup used in measurement of these mixers is depicted in Fig. 5. In this setup, the LO signal with desired AM or PM sidebands has been generated using an HP 83752A synthesizer at a LO power of 9 dBm and the RF signal has been generated using an HP 83711B synthesizer at RF power of -10 dBm. The final IF spectrum with sidebands could be investigated by a spectrum analyzer. In simulations and measurements, LO and RF frequency has been swept keeping their difference at 10 MHz. Thus, the IF frequency is always at 10 MHz.

Near-the-carrier AM(PM) noise rejection has been defined as the difference between LO AM(PM) sidebands power relative to LO power and IF sidebands power relative to IF power. According to the notation defined in Fig. 3, near-the-carrier AM(PM) rejection is defined as

$$\text{AM(PM) rejection (dB)} = \text{LO sideband (dBc)} - \text{IF sideband (dBc)}. \quad (40)$$

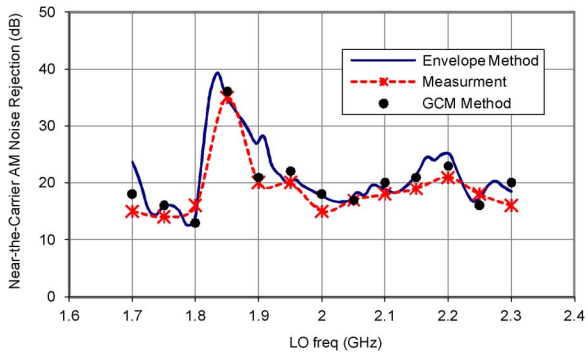

Fig. 6. Near-the-carrier AM noise rejection in rat-race balanced mixer versus the LO frequency.

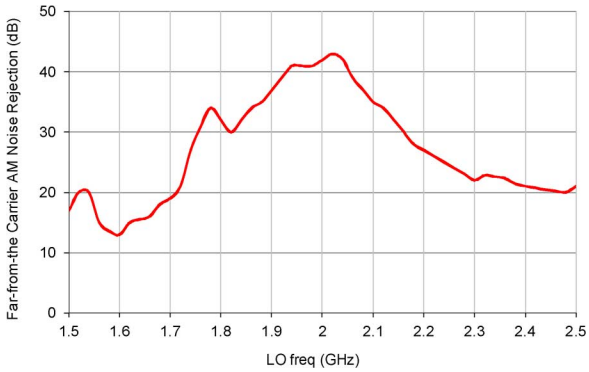

Fig. 7. Far-from-the-carrier AM noise rejection in rat-race balanced mixer.

Calculations of AM and PM rejections are performed separately. As can be inferred from the formulation, IF sidebands are mixing results of the RF signal with LO sidebands and a dc harmonic of $(\partial^2 f(v))/(\partial v^2)$ in (5) and $(\partial^2 Q)/(\partial v^2)$ in (26) (the eighth term in Table I). Since the IF signal is the mixing result of the RF and LO signal, the presented definition for AM (PM) rejection is independent of the RF power (in the RF power range for which the circuit is linear regarding the RF source). By implementing the derived formulation and using the definitions above for a rat-race-coupler-based mixer, near-the-carrier AM rejection is as depicted in Fig. 6. In this figure, the ADS envelope and GCM method results are compared with the measurement. This figure clearly demonstrates the accuracy of the proposed GCM method.

As can be deduced from Fig. 6, near-the-carrier AM noise rejection at a frequency of about 1.85 GHz reaches its maximum value. Contrary to far-from-the-carrier noise rejection (depicted in Fig. 7), near-the-carrier LO noise rejection reaches its maximum in a frequency other than the rat-race center frequency. For this mixer, a plot of conversion loss versus LO frequency is as depicted in Fig. 8, which shows that the mixer conversion loss in a frequency of 1.85 GHz has approximately the same value as 2 GHz.

Another near-the-carrier AM noise rejection simulation has been performed versus LO power in the LO frequency of 1.85 GHz and the results of this simulation and measurement is depicted in Fig. 9. It is seen that above 9 dBm of LO power, we have the maximum rejection.

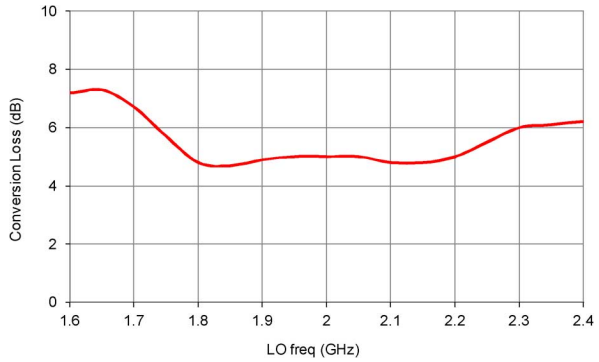

Fig. 8. Conversion loss of rat-race balanced mixer.

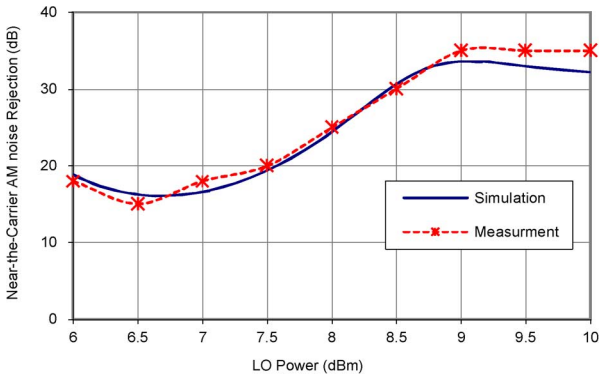

Fig. 9. Near-the-carrier AM noise rejection in rat-race balanced mixer versus the LO Power for LO frequency of 1.85 GHz.

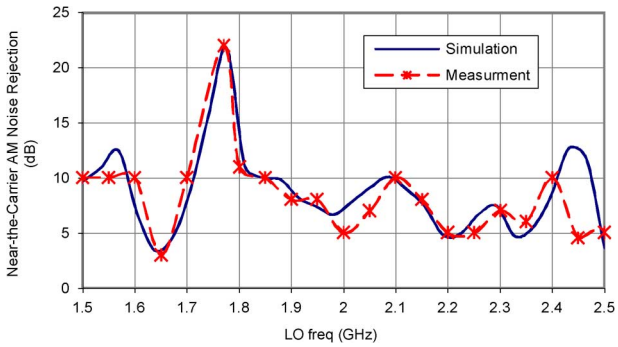

Fig. 10. Near-the-carrier AM noise rejection in branch-line coupler mixer as a function of LO frequency.

This near-the-carrier AM noise rejection in balanced mixers is a result of the symmetrical nonlinearity of diodes used in the mixer.

For a balanced mixer using the branch-line coupler, near-the-carrier AM noise rejection versus LO frequency is depicted in Fig. 10. Similar to previous simulation near-the-carrier AM noise suppression reaches its peak at a frequency other than the coupler center frequency. Thus, for achieving maximum near-the-carrier AM noise rejection in balanced mixers, the LO frequency should not necessarily be the same as the coupler center frequency. For this mixer, near-the-carrier AM noise rejection versus LO power at an LO frequency of 1.75 GHz (the frequency at which near-the-carrier AM rejection reaches its peak value) is plotted in Fig. 11.

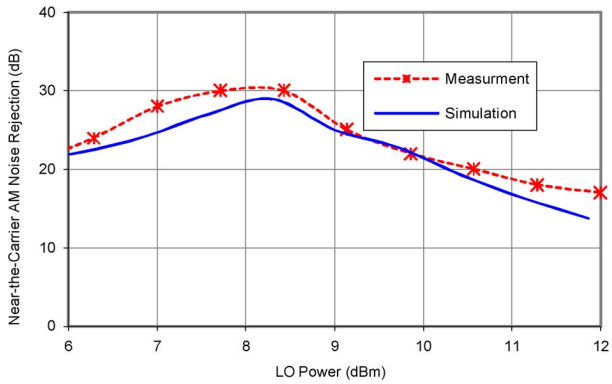

Fig. 11. Near-the-carrier AM noise rejection in branch-line coupler mixer versus LO power for LO frequency of 1.75 GHz.

Furthermore, the phase noise down conversion in all these mixers can be studied by choosing appropriate phases of LO sidebands so that these sidebands make a PM components for the LO. Since there is degree-to-degree translation of phase noise from the RF and LO ports to the IF port [1], there will be no PM noise rejection, as defined above. The simulation using GCM also confirm this fact. Indeed, this is another way for confirmation of validity of the developed simulation program.

IV. Conclusion

A GCM method for computation of noise sidebands in the microwave mixers was presented. In this method, by further expansion of the Taylor series of the nonlinear elements characteristics, a matrix formulation for computation of near-the-carrier noise sidebands of a mixer's down-converted signal is obtained. The method precisely predicts the amount of near-the-carrier AM noise suppression, as it has been demonstrated in a number of practical examples. There is an optimum LO level, as well as an optimum LO frequency for which near-the-carrier AM noise rejection is maximum. This fact was demonstrated computationally and practically. Care must be taken in the design of the balanced mixers as the frequency of maximum near-the-carrier AM noise suppression does not coincide with the design frequency (minimum conversion loss) of the mixer. A sharp peak is generally observed for maximum noise suppression so the designers can manage to obtain that peak of rejection with the help of diode tuning circuits without losing much in the conversion loss.

References

[1] S. A. Mass, *Microwave Mixers*, 2nd ed. Norwood, MA: Artech House, 1986.

[2] R. E. Collin, *Foundation for Microwave Engineering*, 2nd ed. New York: McGraw-Hill, 1992.

[3] K. W. Chang, H. Wang, G. Shreve, J. G. Harrison, M. Core, A. Paxton, M. Yu, C. H. Chan, and G. S. Dow, "Forward-looking automotive radar using the W-band single-chip transceiver," *IEEE Trans. Microw. Theory Tech.*, vol. 43, no. 7, pp. 1659–1668, Jul. 1995.

[4] D. N. Held and A. R. Kerr, "Conversion loss and noise of microwave and millimeter-wave mixers—Part 1—Theory," *IEEE Trans. Microw. Theory Tech.*, vol. MTT-26, no. 2, pp. 49–55, Feb. 1978.

[5] D. N. Held and A. R. Kerr, "Conversion loss and noise of microwave and millimeter-wave mixers—Part 2—Experiment," *IEEE Trans. Microw. Theory Tech.*, vol. MTT-26, no. 2, pp. 55–61, Feb. 1978.

[6] H. Darabi, "A noise cancellation technique in active RF-CMOS mixers," *IEEE J. Solid-State Circuits*, vol. 4, no. 12, pp. 2628–2632, Dec. 2005.

[7] J. Park, C. H. Lee, B. S. Kim, and J. Lasker, "Design and analysis of low flicker noise CMOS mixers for direct conversion receivers," *IEEE Trans. Microw. Theory Tech.*, vol. 54, no. 12, pp. 4372–4380, Dec. 2006.
[8] E. Rubiola and R. Boudot, "The effect of AM noise on correlation phase noise measurements," *IEEE Trans. Ultrason., Ferroelect., Freq. Control*, vol. 54, no. 5, pp. 926–932, May 2007.
[9] V. Rizzoli, D. Masotti, and F. Mastri, "Full nonlinear noise analysis of microwave mixers," in *IEEE MTT-S Int. Microw. Symp. Dig.*, San Diego, CA, May 1994, pp. 961–964.
[10] G. W. Rhyne, M. B. Steer, and B. D. Bates, "Frequency domain nonlinear circuit analysis using generalized power series," *IEEE Trans. Microw. Theory Tech.*, vol. 36, no. 22, pp. 379–387, Feb. 1988.
[11] L. O. Chua and Y. F. Lam, "Decomposition and synthesis of nonlinear n-ports," *IEEE Trans. Circuits Syst.*, vol. CAS-21, no. 5, pp. 661–666, Sep. 1974.
[12] V. Rizzoli, F. Mastri, F. Sgallari, and G. Spaletta, "Harmonic-balance simulation of strongly nonlinear very large-size microwave circuits by inexact newton methods," in *IEEE MTT-S Int. Microw. Symp. Dig.*, 1996, vol. 3, pp. 1357–1360.
[13] V. Rizzoli, "State-of-the-art harmonic-balance simulation of forced nonlinear microwave circuits by the piecewise technique," *IEEE Trans. Microw. Theory Tech.*, vol. 40, no. 1, pp. 12–28, Jan. 1992.
[14] S. A. Mass, *Nonlinear Microwave and RF Circuits*, 2nd ed. Norwood, MA: Artech House, 2003.
[15] S. A. Mass, *Noise in Linear and Nonlinear Circuits*. Norwood, MA: Artech House, 2005.

Ali Kheirdoost was born in Tabriz, Iran, in 1982. He received the B.S. degree in electrical engineering from the Amir Kabir University of Technology, Tehran, Iran, in 2005, and the M.S. degree in electrical engineering from the Sharif University of technology, Tehran, Iran, in 2007.

His major interests include nonlinear microwave circuits, modeling of nonlinear microwave elements, and phased-array antennas.

Ali Banai (M'01) was born in Mashhad, Iran, in 1968. He received the B.S., M.S., and Ph.D. degrees in electrical engineering from the Sharif University of Technology, Tehran, Iran, in 1991, 1994, and 1999, respectively.

Since 1999, he has been as a faculty member with the Department of Electrical Engineering, Sharif University of Technology. His main interests are nonlinear microwave circuits, synchronization of coupled oscillators, and numerical techniques in passive microwave circuits.

Dr. Banai was the corecipient of the Maxwell Premium Award presented at the 2001 IEE Microwave, Antennas, and Propagation Proceedings.

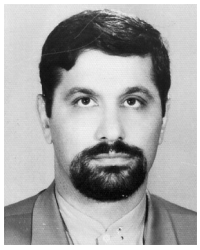

Forouhar Farzaneh (S'82–M'84–SM'96) received the B.S. degree in electrical engineering from the University of Shiraz, Shiraz, Iran, in 1980, the Master degree from the Ecole Nationale Supérieure des Télécommunications (ENST), Paris, France, in 1981, and the DEA and Doctorate degrees from the University of Limoges, Limoges, France, in 1982 and 1985, respectively.

From 1985 to 1989, he was with the Tehran Polytechnic University as an Assistant Professor. Since 1989, he has been with the Sharif University of Technology, Tehran, Iran, where he is currently a Professor of electrical engineering. His main areas of interest are nonlinear microwave circuits and numerical methods associated with their analysis. He has authored or coauthored numerous journal and conference papers in the field of microwave and millimeter-wave circuits. He has also authored a book (in Persian) about RF circuit design.

Dr. Farzaneh was a corecipient of the 1985 European Microwave Prize. He was also the recipient of the Maxwell Premium award presented at the 2001 IEE Microwave, Antennas and Propagation Proceedings.